AD-A158 231 THE INFLUENCE OF THE HELIOSPHERIC CURRENT SHEET AND ANGULAR SEPARATION ON.. (U) STANFORD UNIV CA CENTER FOR SPACE SCIENCE AND ASTROPHYSICS H M HENNING ET AL. 1/1

UNCLASSIFIED APR 85 CSSA-ASTRO-85-17 N00014-76-C-0207 F/G 20/3 NL

END

DATE FILMED 10 85

DTIC

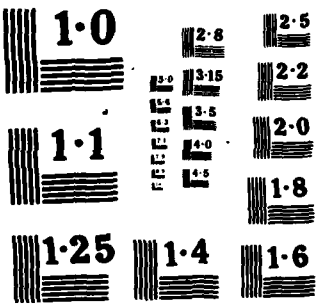
1·0
1·1
1·25
2·8
3·15
3·5
4·0
4·5
2·5
2·2
2·0
1·8
1·4
1·6

The Influence of the Heliospheric Current Sheet and Angular Separation on Flare Accelerated Solar Wind

Harald M. Henning, Philip H. Scherrer and J. Todd Hoeksema

Center for Space Science and Astrophysics

Stanford University, Stanford, CA

The Influence of the Heliospheric Current Sheet and Angular Separation on Flare Accelerated Solar Wind

Harald M. Henning, Philip H. Scherrer and J. Todd Hoeksema

Center for Space Science and Astrophysics

Stanford University, Stanford, CA

CSSA-ASTRO-85-17

April 1985

Submitted to: Journal of Geophysical Research

Office of Naval Research Contract N00014-76-C-0207

National Aeronautics and Space Administration Grant NGR5-020-559

National Science Foundation Grant ATM77-20580

Abstract. *A complete set of major flares has been used to investigate the effect of the* heliospheric current sheet on the magnitude of the flare-associated disturbance measured at Earth. It was found that disturbances associated with flares located on the same side of the current sheet as Earth were of larger magnitude than those associated with flares located such that the flare-accelerated material would have to cross the current sheet. It was also found that the angular separation between the flare position and Earth has a strong effect on the magnitude of the disturbance. A larger angular separation tended to result in a smaller disturbance. Thirdly, it was determined that flares tend to occur near the heliospheric current sheet.

1. Introduction

It is known that flares produce disturbances in the solar wind resulting in geomagnetic activity at Earth. However, the magnitude of such disturbances cannot yet be predicted for any given flare. This paper presents the results of a statistical analysis which separates and identifies some of the quantities which determine the relative magnitude of a flare-associated disturbance. The main thrust of the analysis is to determine the effect of the relationship between the location of the flare and the location of the heliospheric current sheet (HCS). To avoid bias in the estimate of an HCS effect, however, one must also examine any effect due to the position of the flare on the solar disk. This analysis produces two major results: First, that flares occurring on the opposite side of the HCS from the earth produce smaller solar wind and geomagnetic disturbances than those on the same side. Second, we find that the disturbance decreases with increasing angular distance of the flare from the sub-earth point.

Three kinds of data were used in the present study. The first is the list of major flares as defined by Dodson and Hedeman (1971, 1975, 1981). The second is the location of the HCS as computed by Hoeksema (1982, 1983, 1984, 1985). The third is the indicator of solar wind response to the flare, and has been taken to be the geomagnetic disturbance index D_{ST} and solar wind velocity when available.

2. Data

The flares used in this analysis are taken from the UAG reports of the Comprehensive Flare Index (CFI) compiled by Helen W. Dodson and E. Ruth Hedeman (1971, 1975, 1981). These records contain a complete list of all observed major flares from 1955-1979. The CFI is comprised of five components:

1) Importance of ionizing radiation as indicated by time-associated Short Wave Fade or Sudden Ionospheric Disturbance (Scale 0-3).

2) Importance of Hα flare (Scale 0-3).

3) Magnitude of $\approx 10cm$ flux; (characteristic of log of flux in units of $10^{-22} Wm^{-2}Hz^{-1}$); (Scale 0-4).

4) Dynamic spectrum; (Type II = 1, Continuum = 2, Type IV with duration > 10 min = 3); (Scale 0-3).

5) Magnitude of ca. $200MHz$ flux; (characteristic of log of flux in units of $10^{-22} Wm^{-2}Hz^{-1}$); (Scale 0-5).

The total CFI of a flare is then just the sum of the 5 components, with a possible range of 1 to 18.

A major flare is defined as one which was well above average in either ionizing, $H\alpha$, or radio frequency radiation (corresponding CFI component ≥ 3), or exhibited a Type II burst or Type IV burst with longer than 10 min duration (Dodson and Hedeman 1971, 1975, 1981). From this still formidable list the data for this analysis was selected by including only flares with a total CFI of 7 or greater. For the interval from 1968 through 1979 the data includes 505 flares. Missing data for the flare position or solar wind parameters reduces this number to slightly more than 400. All these flares were used for the part of the analysis determining the disk-position dependence of solar wind disturbances.

The location of the heliospheric current sheet (HCS) is derived from the potential field model calculations done at Stanford (Hoeksema 1982, 1983, 1984, 1985). The HCS data starts

in the middle of 1976, and continues to the present. For the HCS analysis then, the flares from 1976 to 1979 were used. The majority of these occurred in 1978 and 1979, as the solar cycle maximum was approaching. There are 181 flares in this interval, of which slightly more than 140 remain after elimination of those with missing positions or solar wind data.

The geomagnetic index D_{ST}, which is continuously available and proportional to solar wind speed and B_z (Murayama 1982), and the solar wind speed hourly averages observed by ISEE3 are used to measure the flare generated disturbance. Figures 1 and 2 show superposed epoch analyses of solar wind speed and D_{ST} about flare times. These plots show a strong peak in the disturbance of the solar wind and D_{ST} 2 to 4 days after the flare. Note that a higher value for solar wind speed is the signature of a disturbance, whereas for D_{ST} it is a lower, i.e. greater negative, value. We chose to examine 24-hour averages of these two indices to study the effect of flare position on the disk and relative to the HCS. Use of the 24-hour averages has the advantage that it avoids the subjectivity that occurs when one attempts to identify the source of a particular disturbance. An analysis of 24-hour intervals in the period from 1.0 to 4.5 days after the flare showed that averages of the interval from 2.0 to 3.0 days after the flare demonstrate the effect of the HCS and flare position most strongly. We found that there was a strong HCS effect evident when examining any 24-hour interval between 1.5 and 4.5 days after the flare, beginning sharply at 1.5 days and a gradual decrease commencing 3 days after the flare and continuing past 4.5 days. Thus, for each flare in our study, a 24 hour average was calculated for the interval starting 2 days after the flare.

The time interval chosen allows for a propagation velocity of the flare-accelerated material ranging from 577 km/sec to 866 km/sec. Note that the 24 hour average of the solar wind speed itself will usually be substantially less than this, since the average also includes quiet solar wind. Very likely some of the flare associated disturbances may be missed, but, without making the time intervals too large and further diluting the size of a disturbance, this problem cannot be avoided in a completely objective analysis where we want to avoid the uncertainty in associating a specific solar wind or D_{ST} disturbance with a particular flare.

3. Analysis

3.1. The Heliospheric Current Sheet

To determine whether a flare-associated disturbance had to cross the HCS to reach Earth we looked at the source surface calculated at Stanford with the potential field model (Hoeksema 1982, 1983, 1984, 1985). We assume the steady, undisturbed solar wind carries the magnetic structure of the source surface into interplanetary space, reaching Earth after an average of 5 days. The flare material is assumed to take an average of 2.5 days to reach Earth. Thus we can estimate the magnetic structure at the flare position on the sun and at Earth when the disturbance arrives. Specifically, if the polarities of the magnetic field (either inward directed or outward directed) are different, the flare is considered to be on the opposite side of the HCS, i.e. the flare material has to cross the HCS to reach Earth. If the polarities are the same, the flare is considered to be on the same side of the HCS. If either of the positions was very close to the HCS, i.e. the field magnitude was very small (less than $0.1\mu T$ on the source surface), the flare was eliminated from the analysis. There were four such instances. In addition, two cases where the flare material would have propagated tangential to the HCS were eliminated from the study, since the latitudinal extent of the HCS is uncertain by a few degrees. There were three cases where flare material had to cross two HCS's. The final flare set for the solar wind speed analysis contains 135 flares, of which 75 are on the same side of the HCS and 60 on the opposite side. There were 2 more flares in each category available for the D_{ST} analysis.

We define a quantity D, which we call the difference measure, that provides an indication of the significance of the effect the HCS has on flare-associated disturbances as follows :

$$D = \frac{(\bar{X}_{same} - \bar{X}_{opp})}{(\sigma_{X_{same}} + \sigma_{X_{opp}})},$$

where X is the quantity with which we are measuring the disturbance, e.g. solar wind speed 3-4 days after the flare.

In words, D is the difference between the average quantity (solar wind speed, D_{ST}) for flares on the same side of the HCS and the average quantity for flares on the opposite side of the HCS, as measured in units of the average error of the mean. Thus, a large absolute value of D is an indicator of an effect.

Figure 3 shows the values of D for solar wind speed 2 to 3 days after the flare. Large positive D means a significantly larger value of average solar wind speed for flares on the same side of the HCS than for flares on the opposite side. In panels a-e the flares were grouped depending on their value for different components of the CFI. The flares in figure 3a were grouped by the value of the first component of the CFI, i.e. by the importance of ionizing radiation. The value of D for all flares which had ionizing radiation importance of 1 or greater is shown at the abscissa "1+", the value of D for all flares with ionizing radiation importance of 2 or greater at abscissa "2+", and so on. Similarly, figure 3b was grouped by Hα importance, 3c by the magnitude of $10cm$ flux, 3d by the dynamic spectrum, and 3e by the magnitude of $200MHz$ flux. Note that the first point in each panel includes all flares with a CFI component value of 0 or greater, i.e. all flares in the data. The reason for this method of grouping is that since flares are selected on the basis of a value of total CFI ≥ 7, a value of 0 in one component of the CFI implies on the average a high value in another component of the CFI. This bias prevents us from examining flares grouped by a particular value of a particular CFI component, rather we examine flares grouped according to whether a CFI component exceeds a given threshold. The adopted grouping enables one to see better the effect large flares have as opposed to smaller ones.

In the final panel, f, flares were categorized by their total CFI value, in the method described above.

Figure 4 has the same format as figure 3, but shows the response of D_{ST} rather than the solar wind speed. In this figure, a large negative value of D indicates an effect, since a more negative value of the D_{ST} index indicates greater geomagnetic activity.

The first and most important thing to be learned from these plots is that there is a definite HCS effect. The flares on the same side of the HCS as the earth result in a larger disturbance, i.e. greater solar wind speed and more negative D_{ST}. The size of this effect is quite large, on the order of 4σ (solar wind speed) or 5σ (D_{ST}), which corresponds to about a 55 km/sec difference in solar wind speed or 18 in D_{ST} units. In order to check for consistency of the effect, the flares were divided into two time intervals and the calculations done separately for each. The resulting plots were practically identical to each other and to the calculations from the full data (figures 3 and 4), demonstrating the consistency convincingly.

None of the components of CFI, nor the total CFI, seems to produce a significantly larger or smaller effect. All the plots look fairly similar, even though for each panel different flares determined the points for CFI component values greater than 0. Thus none of the components of CFI stands out as a determinant for whether a flare will cause a large disturbance or not. Nor does total CFI provide a better organization, although it certainly provides a more complete list of major flares than any of its separate components.

One is tempted to note that in almost all panels, for a higher value of the CFI component the absolute value of D is getting smaller, i.e. perhaps for the truly strongest flares the HCS effect is less. However, another factor contributes to produce this decrease in D. This factor is the definition of D. For the points at larger values of the CFI component there are fewer flares, and thus the error of the mean is larger, giving a smaller value of D. If one examines the actual solar wind speed or D_{ST} difference between the average for flares on the same side and the average for flares on the opposite side, the tendency is actually for the difference to be a larger number. Therefore, contrary to the immediate assumption, it appears that the HCS effect is proportionally stronger for stronger flares. However, the uncertainty of the numbers, as demonstrated by the decrease of D in the plots, means that we cannot provide a concrete answer to this question about large flares.

Summarizing this section, by use of these graphs we have successfully demonstrated that there exists an HCS effect, given an idea of its significance and determined that no component of CFI, i.e. no energy range, stands out as a strong organizer of solar wind disturbances.

3.2. Angular Separation

In the preceding analysis, we found that the position of the flare with respect to the HCS, i.e. same or opposite side, resulted in a significant difference in the size of the flare-associated disturbance. However, to get an unbiased estimate of an effect the HCS has on such disturbances one has to consider a possible systematic effect associated with the angular distance of the flare from the sub-earth position. It is clear that the farther a flare is separated in angular distance from the sub-earth point, the more likely it is that an HCS lies in-between. Thus there is a likely systematic bias that disturbances which have to cross the HCS are due to flares which are at larger angular distances from Earth. We have examined the solar wind response at Earth to a flare as a function of the angular distance between the flare and the sub-earth point. In addition to later enabling us, in our main analysis, to separate the HCS effect from this distance effect, this investigation is, of course, interesting in its own right.

As a first test of the systematic bias, we found that indeed, for the period starting in 1976, where the HCS position is known, and ending in 1979, the end of the CFI compilation, the average angular distance from Earth for flares on the same side of the HCS was 42°, while for those on the opposite side it was 57°.

To judge the effect of this bias we examined the dependence of the solar wind response, as measured by magnitude of solar wind speed or D_{ST}, on the angular separation between the flare and Earth. Since we are not restricted by having to know the location of the HCS, we have taken all flares in our data with known positions, starting with the year 1968 and running through 1979. The angular distance to the sub-earth point at the average time when flare material is assumed to reach Earth, i.e. after 2.5 days, was calculated

for each flare. The flares were then binned by distance and the average solar wind speed and D_{ST} plotted in figures 5a and 6a respectively. Figures 5b and 6b show the results of a similar calculation, except that only longitudinal separation was considered.

The graphs clearly show an effect on the average size of the disturbance. The farther Earth is separated in angular distance from the position of the flare, the weaker the disturbance measured at Earth. It is debatable whether the dependence is a monotonic decrease of the disturbance with angular distance, or whether there is a region of about $\pm 40^{\circ}$ around the flare position where the disturbance is large, and outside of this "bubble" the effect of the flare is much smaller (especially evident for D_{ST}). However, the scatter plot of all flares seems to support a monotonic decrease.

Also, one can argue that there seems to be an East-West asymmetry. For positive longitudinal separation the average magnitude of a disturbance, as measured by high solar wind speed or large negative D_{ST}, seems larger than for corresponding negative longitudinal separation. Thus, it suggests that a flare on the western hemisphere of the sun may have a larger effect than one on the eastern hemisphere. This is consistent with the report that streams from flares on the western hemisphere have a speed 50% higher than those from eastern flares (Pudovkin et al 1979). However, since the uncertainty is fairly large we will consider only the angular distance in the further analysis.

If we assume a roughly linear monotonic decrease, then we can estimate the size of the systematic effect introduced into our HCS analysis. We calculated the average angular distance for flares on the same side of the HCS, 42°, and the opposite side, 57°. Figure 5a shows a difference of about 15 km/sec in average solar wind speed between these two values. Figure 6a provides the same information for D_{ST}, a difference of about 3 D_{ST} units.

3.3. The HCS Effect

Returning to our main investigation of the effect of the HCS on the disturbances caused by flares, we must try to remove the effect of angular distance. To do so, a straight

line was fitted to a plot of disturbance (as measured by solar wind speed or D_{ST} measured at Earth 2.0 to 3.0 days after the flare) vs. angular separation for all flares used in the HCS analysis (figures 7a and 7b). These lines then represents the effect of angular distance, although one cannot totally separate the effects since at larger angular distance there are more flares on the opposite side of the HCS, and vice versa for smaller angular distance, influencing the slope of the line such that the HCS effect is weakened by an unknown, although certainly little, amount. In the next step the flares were separated according to whether they were on the same or opposite side of the HCS. For each flare the distance from the line (in appropriate units, i.e. km/sec for solar wind speed, or D_{ST} units) was calculated. Each group, i.e. same and opposite side flares, has a roughly Gaussian distribution. The centroid and error of the mean of these distributions were calculated for both groups of flares. Then the difference between the centroid for flares on the same side of the HCS and the centroid for flares on the opposite side was taken, producing the following results :

$$Solar\ Wind\ Speed\ :\ \overline{same} - \overline{opp.} = 43.4 \pm 19.5\ km/sec\ \ (98.7\% > 0)$$

$$D_{ST}\ :\ \overline{same} - \overline{opp.} = -15.4 \pm 4.6\ \ (99.9\% < 0)$$

Referring to the values quoted in section 3.1 and 3.2, one sees that the angular distance effect accounts for roughly one fourth of the difference demonstrated in figures 1 and 2. The other three fourths result from the HCS effect.

3.4. Distance from the HCS

As an aside resulting from this analysis, the distance of each flare from the nearest HCS was calculated, giving an average of 16° for flares from September of 1977 to the end of 1979, a period of continuous high activity. There was no significant difference between the average distance for flares on the same side of the HCS and the average distance for those on the opposite side. A set of artificial flare positions was then determined by keeping the actual latitudes (to insure a realistic distribution in latitude) but assigning random Carrington longitudes within this interval. Then the average distance to the HCS for this

set was calculated. This process was repeated 400 times. In none of these 400 trials did the average come as low as the true average, the lowest being only 17.5°. The overall average distance between random positions and the HCS for all iterations was 21°. This average is significantly greater than the average resulting from the true flare position. This confirms the tendency for flares to occur near the HCS (Dittmer 1975).

4. Conclusion

In this analysis we have investigated the effect of angular separation and the HCS on flare associated disturbances measured at Earth. We have found that there is a clear association between proximity of the flare to the sub-earth point and stronger disturbances. This relation accounts for a fourth of the difference noted between disturbances from flares on the same and opposite sides of the HCS. A strong effect associated solely with the HCS remains at a greater than 98% confidence level. Flares on the same side of the HCS tend to produce larger disturbances than flares on the opposite side. This influence of the HCS may be explained by the fact that solar wind speed tends to be at a minimum along the HCS (Borrini 1981), and thus disturbances in propagating to Earth would have to interact with this slower plasma, perhaps weakening them.

5. References

Borrini, G., Wilcox, J. M., Gosling, J. T., Bame, S. J. and Feldman, W. C.: Solar Wind Helium and Hydrogen Structure Near the Heliospheric Current Sheet: A Signal of Coronal Streamers at 1AU, *J. Geophys. Res.* **86**, 1981, 4565-4573.

Dittmer, P. H.: The Relationship between Solar Flares and Solar Sector Boundaries, *Solar Physics* **41**, 1975, 227-231.

Dodson, H. W. and Hedeman, E. R.: An Experimental Comprehensive Flare Index and its Derivation for "Major" Flares, 1955-1969, *Report UAG-14*, 1971.

Dodson, H. W. and Hedeman, E. R.: Experimental Comprehensive Solar Flare Indices for Certain Flares, 1970-1974, *Report UAG-52*, 1975.

Dodson, H. W. and Hedeman, E. R.: Experimental Comprehensive Solar Flare Indices for "Major" and Certain Lesser Flares, 1975-1979, *Report UAG-80*, 1981.

Hoeksema, J. T., Wilcox, J. M. and Scherrer, P. H.: Structure of the Heliospheric Current Sheet in the Early Portion of Sunspot Cycle 21, *J. Geophys. Res.* **87**, 1982, 10331.

Hoeksema, J. T., Wilcox, J. M. and Scherrer, P. H.: The Structure of the Heliospheric Current Sheet: 1978 - 1982, *J. Geophys. Res.* **88**, 1983, 9910.

Hoeksema, J. T.: Structure and Evolution of the Large Scale Solar and Heliospheric Magnetic Fields, CSSA-ASTRO-84-07, Ph.D. Thesis, 1984.

Hoeksema, J. T. and Scherrer, P. H.: An Atlas of Photospheric Magnetic Field Observations and Computed Heliospheric Magnetic Fields from the John M. Wilcox Solar Observatory at Stanford 1976-1984, CSSA-ASTRO-85-11, 1985.

Murayama, T.: Coupling Function Between Solar Wind Parameters and Geomagnetic Indices, *Rev. Geophys. and Space Phys.* **20**, 1982, 623.

Pudovkin, M. I., Zaitseva, S. A. and Benevolenska, E. E..: The Structure and Parameters of Flare Streams, *J. Geophys. Res.* **84**, 1979, 6649.

6. Acknowledgements

We wish to thank Bill Merryfield and Steve Suess for helpful contributions and discussions. This work was inspired by John Wilcox.

This work was supported in part by the Office of Naval Research under Contract N00014-76-C-0207, by the National Aeronautics and Space Administration under Grant NGR5-020-559, and by the Atmospheric Sciences Section of the National Science Foundation under Grant ATM77-20580.

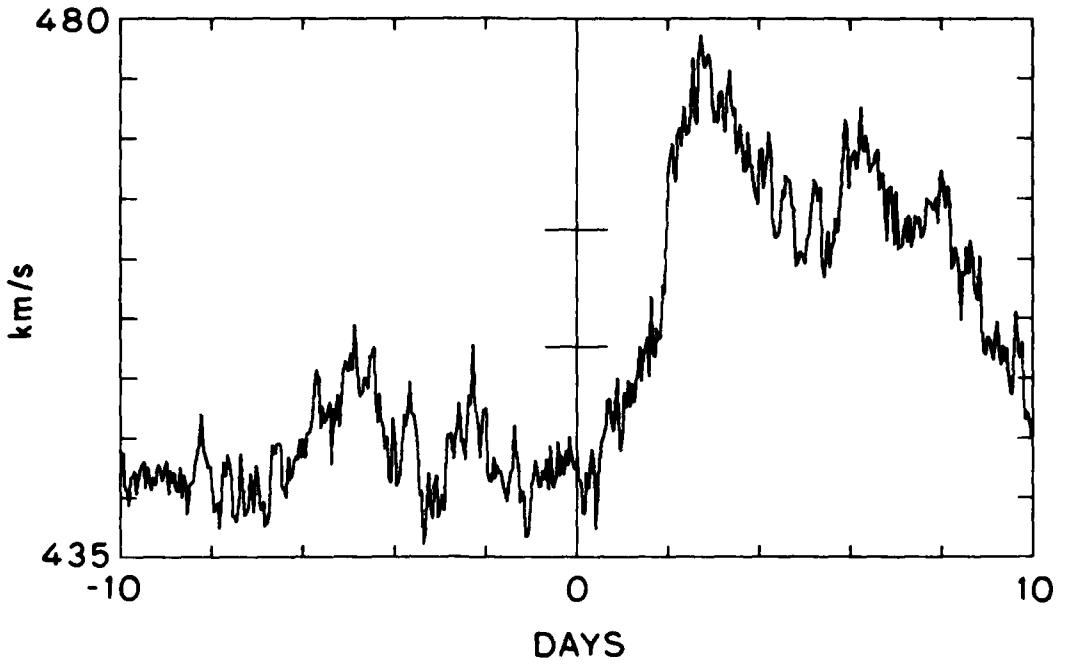

Fig.1. Superposed epoch plot of solar wind speed at Earth around flare times (day 0). A strong peak is evident between 2 and 4 days after a flare. The second peak between 5 and 8 days, as well as the peaks before the flare can be attributed to the fact that flares tend to occur in bunches, so that these peaks are signatures of flares before and after the one at day 0.

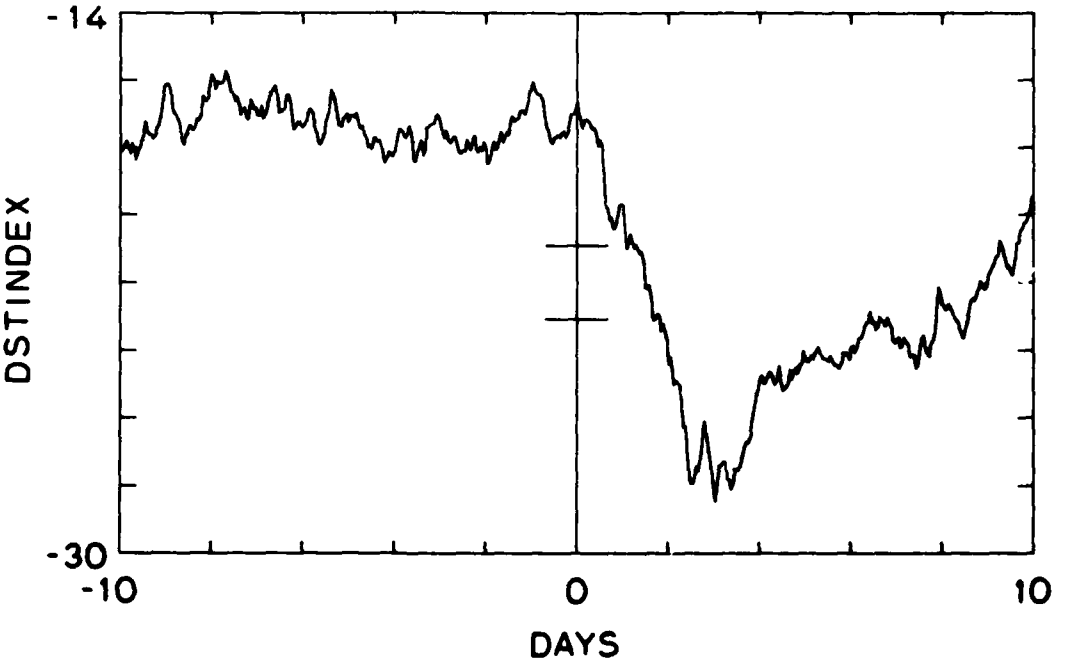

Fig.2. The same as figure 1, but for D_{ST} rather than solar wind speed. The size of the peak in activity (dip in D_{ST}) is relatively greater than for solar wind speed.

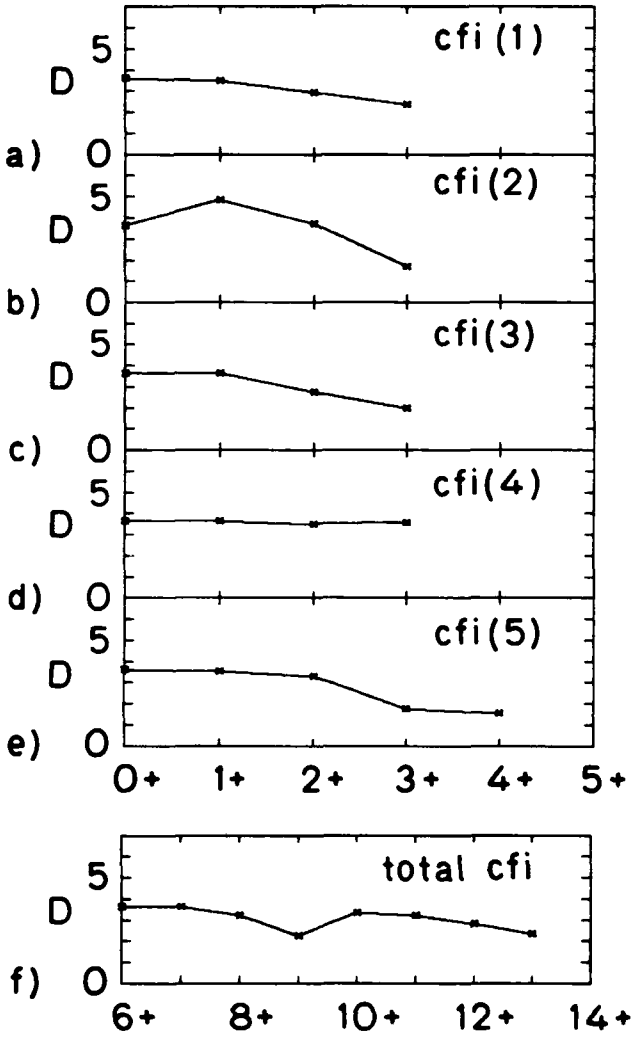

Fig.3. Graphs of the difference measure D for solar wind speed vs. magnitude of the flare as measured with a) importance of ionizing radiation, b) importance of H_α flare, c) magnitude of $10cm$ flux, d) dynamic spectrum, e) magnitude of $200Hz$ flux, and f) total CFI. In each panel, D runs from 0 (bottom) to 7 (top).

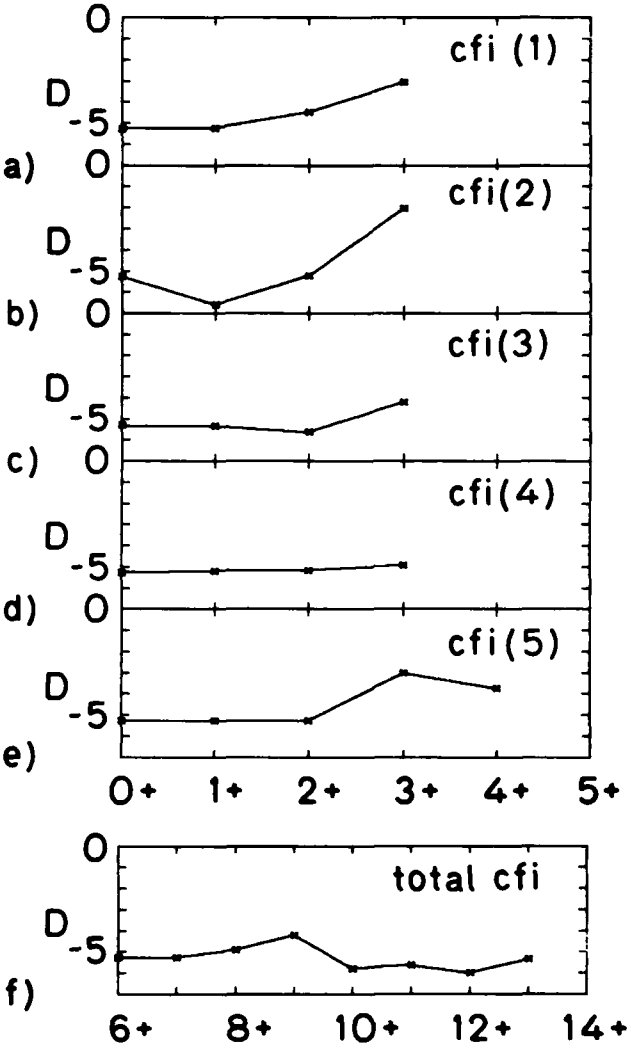

Fig.4. The same as figure 3, but for D_{ST} rather than solar wind speed. The magnitude of D is greater than for solar wind speed, otherwise the graphs are very similar. In each panel, D runs from -7 (bottom) to 0 (top).

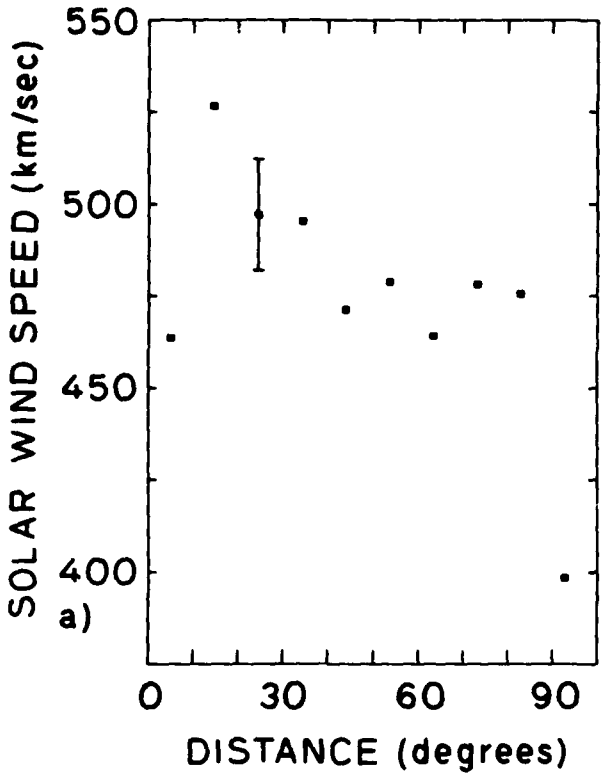

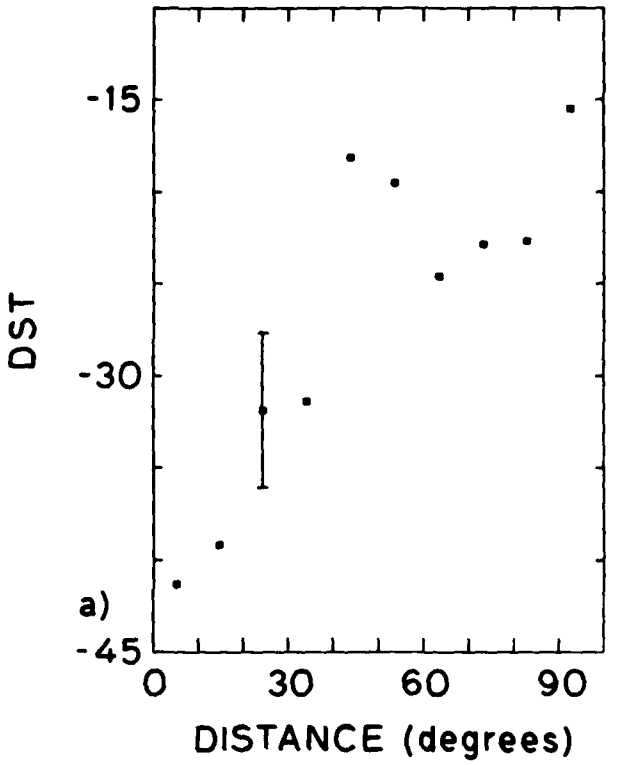

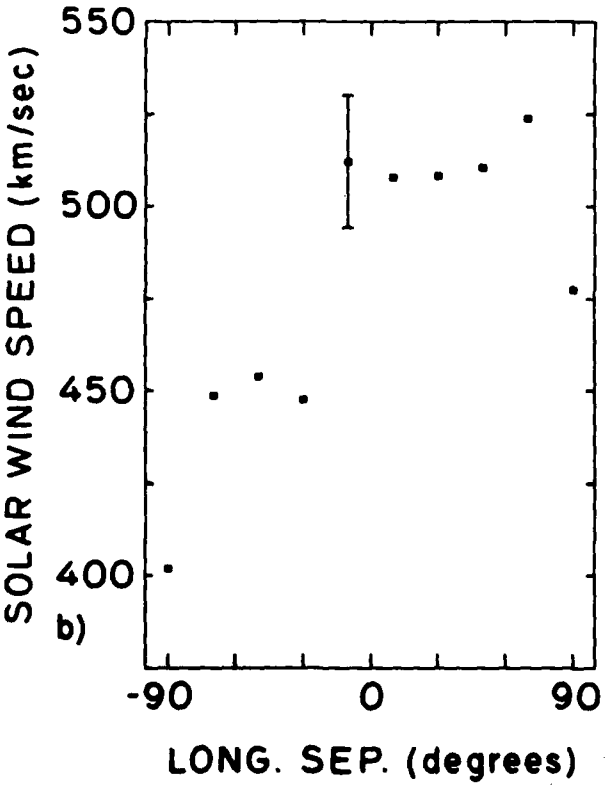

Fig.5. Plots of the average solar wind speed 2 to 3 days after a flare vs. a) angular distance from the subearth point and b) longitudinal seperation from the subearth point. Note the apparent strong east-west asymetry in b).

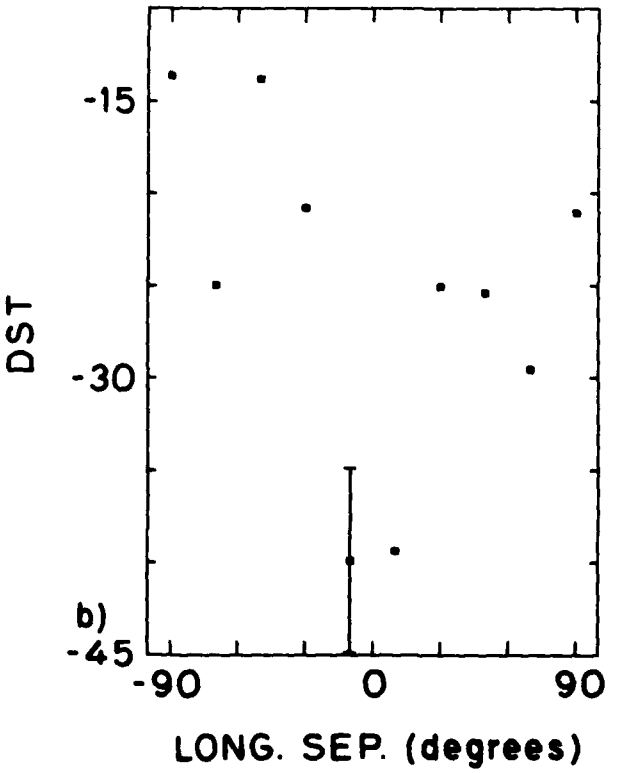

Fig.6. The same as figure 5, but for D_{ST} rather than solar wind speed. Note the lack of a strong east-west asymetry in b).

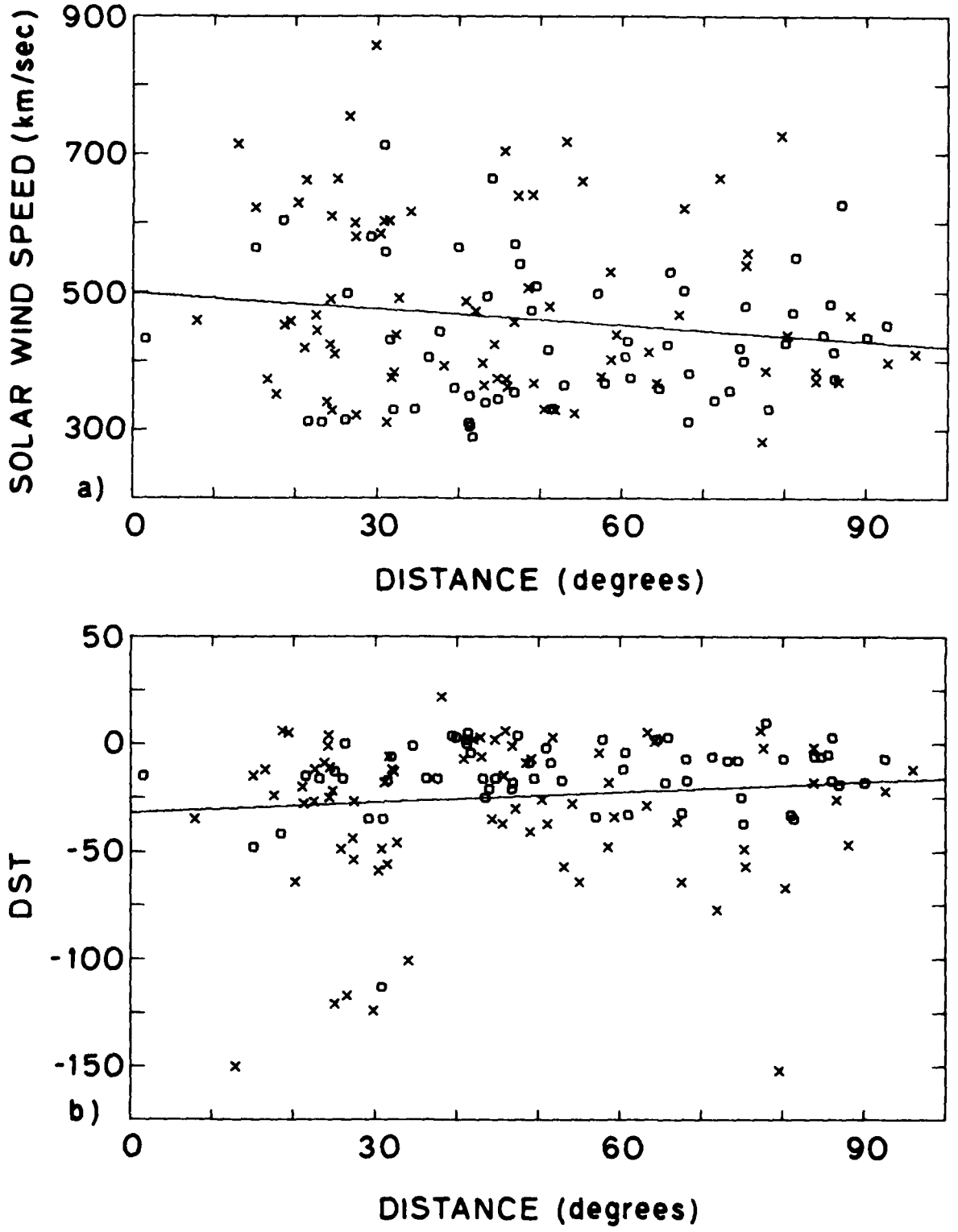

Fig.7. Graphs of a) solar wind speed and b) D_{ST} 2 to 3 days after a flare vs. angular distance. The line is a least squares fit to all points, and represents the effect of angular distance on the magnitude of the flare disturbance. Flares occuring on the opposite side of the HCS from Earth are marked with an *o*, those on the same side with an *x*.

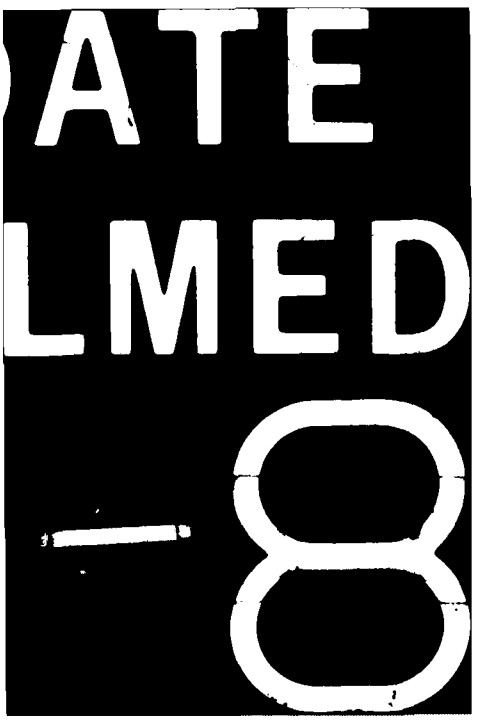
ATE
LMED
8